In Vivo Mouse Imaging and Spectroscopy in Drug Discovery

Nicolau Beckmann, Catherine Cannet, Martin Rausch, Rainer Kneuer, and Hans-Ulrich Gremlich

Introduction

The knowledge about the pathophysiology of a disease as well as its early diagnosis and characterization stands at the center of drug research. The better the mechanisms of a disease known, the higher the probability of finding an appropriate therapy. Also, the better and earlier a disease can be diagnosed and characterized, the greater will be the chance to interfere in the pathological process with a chemical entity. This reasoning sets the framework for the use of imaging in pharmaceutical research.

In a simplified view, the drug discovery and development process can be divided into four phases (Fig. 1). In vivo imaging may play an important role in three of these phases. In target validation and pre-clinical research, which encompasses all endeavors previous to testing compounds in humans, a significant portion of the in vivo activities is performed in mice. Since mouse and man are similar at the genetic level, it is possible to measure similar disease parameters in mice and in humans. The ability to manipulate the mouse genome has allowed and will allow us to define molecular pathways describing the processes of disease initiation and progression. These models may serve as an excellent platform for the identification of novel molecular targets for therapy as well as for the evaluation of the efficacy of targeted therapies. Indeed, genetic alterations in the mouse often result in functional changes through which relevant pharmacological effects in man can be predicted (Tornell and Snaith 2002; Zambrowicz and Sands 2003; Zambrowicz et al. 2003). A retrospective evaluation of the knockout phenotypes for the targets of the 100 best-selling drugs indicates that effects in murine models of human disease correlate well with known clinical drug efficacy (Zambrowicz and Sands 2003), suggesting a productive path forward for discovering future drug targets.

N. Beckmann (✉)
Global Imaging Group, Novartis Institutes for BioMedical Research,
Forum 1, Novartis Campus, CH-4056, Basel, Switzerland
e-mail: nicolau.beckmann@novartis.com

D. Borsook et al. (eds.), *Imaging in CNS Drug Discovery and Development: Implications for Disease and Therapy*,
DOI 10.1007/978-1-4419-0134-7_15, © Springer Science+Business Media, LLC 2010

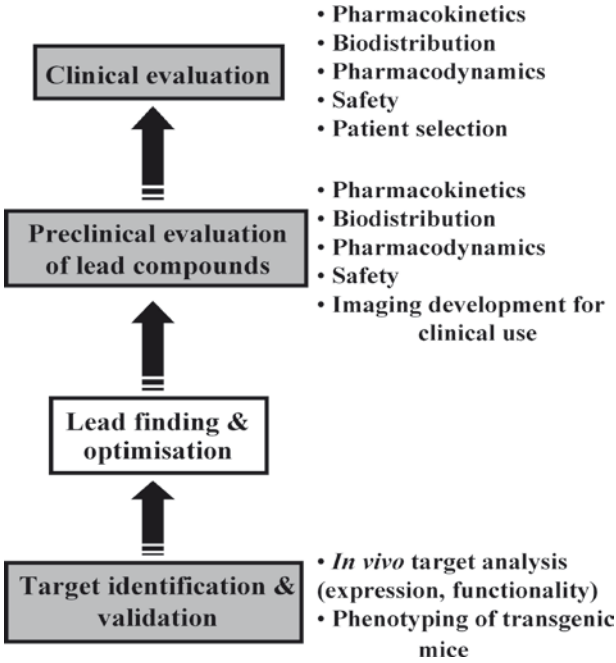

Fig. 1 Simplified view of the drug discovery process. Except for the lead finding and optimization phase, possible uses of in vivo imaging at the several phases are indicated on the right

In this chapter, we discuss the use of mouse imaging in the context of drug discovery. First, a brief description of imaging techniques currently adopted for imaging mice is provided. The design of imaging probes, which is becoming more and more important in this context, is addressed next. Then, we turn our attention to the specific roles played by transgenic mice in drug discovery. Finally, we present examples of mouse imaging in Alzheimer's research, selected to illustrate some key points reflecting the advantages, challenges and limitations of in vivo imaging in preclinical drug research.

Techniques for in Vivo Brain Imaging and Spectroscopy of Mice

An overview of current imaging modalities of interest within drug research is provided in Table 1. In this section we briefly outline the main characteristics of these techniques, for the scope of imaging mice in vivo. The reader is referred to other reviews to obtain more detailed information on mouse imaging methods including practical aspects and challenges (Acton and Kung 2003; Chen and Henkelman 2006; Contag and Bachmann 2002; Gambhir 2002; Hammoud et al. 2007; Nieman et al. 2007; Ntziachristos et al. 2003; Ritman 2004; Rudin 2006).

Table 1 Current imaging modalities of interest in drug research and discovery

Technique	Spatial resolution; time scale	Clinical imaging	Application	Main characteristics
Ultrasound	50 μm; s to min	Yes	Anatomical, functional; drug delivery	Microbubbles as contrast agent; difficult to image through bone or lungs
CT	50–100 μm; s to min	Yes	Anatomical, functional	Poor soft tissue contrast
MRI	80–100 μm; s to min	Yes	Anatomical, functional, metabolic, cellular	High spatial resolution and soft tissue contrast; low sensitivity (~1 mmol)
PET (high energy γ-rays)	1–2 mm; min	Yes	Metabolic, functional, molecular	Most common isotopes have short half-lives; high sensitivity (pmolar concentrations); cyclotron needed
SPECT (low energy γ-rays)	1–2 mm; min	Yes	Functional, molecular	Radioisotopes have longer half-lives than those used in PET; sensitivity 10–100 times lower than PET
Bioluminescence	1–3 mm; s to min	No	Molecular	High sensitivity (~1 nmol); transgene based approach; light emission prone to attenuation with increasing tissue depth
NIRF	1–3 mm; s to min	Yes[1]	Molecular, functional	High sensitivity (~1 nmol); excitation and emission light prone to attenuation with increased tissue depth

[1]Applications in clinical evaluation of breast cancer and arthritis under evaluation

Ultrasound and Drug Delivery to the Brain

The central nervous system (CNS) is protected from the entry of foreign substances by the almost impenetrable blood–brain barrier (BBB), which hampers the delivery of potentially effective diagnostic or therapeutic agents. Because antibody-based agents with a molecular size of approximately 150 kDa are easily blocked by the BBB, their delivery to the CNS requires the temporary suspension of the physiological role of the BBB to bar larger molecules from the CNS.

Advances in acoustic technology have made ultrasound a modality with therapeutic as well as diagnostic applicability. The combined use of ultrasound and gas bubble-based ultrasound contrast agents induces bioeffects, such as transient changes in cell-membrane permeability (Kinoshita and Hynynen 2005). This approach has been shown to facilitate the reliable disruption of the BBB in murine models (Choi et al. 2007; Kinoshita et al. 2006a). The technique has been applied to examine in mice the feasibility of delivering Herceptin through the BBB (Kinoshita et al. 2006b) (Fig. 2). Contrast-enhanced high-resolution magnetic resonance imaging (MRI) revealed BBB opening.

Microcomputerized Tomography

Microcomputerized Tomography (micro-CT) systems providing high-resolution images (~50 μm) and rapid data acquisition (typically 5–30 min) are emerging as a cost-effective means for detecting soft-tissue structures, skeletal abnormalities and tumors in small animals (Badea et al. 2004; Cavanaugh et al. 2004; Ford et al. 2005; Ritman 2004). The use of iodinated contrast agents enhances the weak endogenous contrast between different soft tissues. However, the difficulty in designing CT contrast agents limits the utility of the technique for molecular imaging applications, and at least in the near future, micro-CT will be used essentially to supplement data from other molecular imaging techniques.

Fig. 2 Experimental settings and BBB disruption in mice by MRI-guided focused ultrasound. (**a**) Diagram and protocol for BBB opening used in this experiment. Mice in the supine position were placed on the sonication table in the MR scanner. The ultrasound beam was focused through the intact skull on the target in the brain. (**b**) Representative example with BBB disruption achieved by 0.6-MPa (peak negative-pressure amplitude) focused ultrasound exposure. (*Upper*) The BBB opening was easily monitored by leakage of the MR contrast agent into the brain parenchyma on axial (AX) and coronal (COR) MR images (*arrows*). (*Lower Left*) The location of the BBB opening was confirmed by trypan blue staining of the affected area. (*Lower Right*) No apparent macroscopic damage related to BBB disruption can be seen. (**c**) Magnitude of BBB disruption in the animal presented in B monitored by the MR-intensity change. Absolute values of the MR intensity of the sonicated target (*open circle*) and the contralateral side (control; *filled circle*) are plotted for repeated image acquisitions after sonication. Data are presented as the mean ± SD of four voxels. Courtesy of Kullervo Hynynen, Harvard University, Boston. Reproduced with permission from Kinoshita et al. (2006b). © 2006 The National Academy of Sciences of the USA

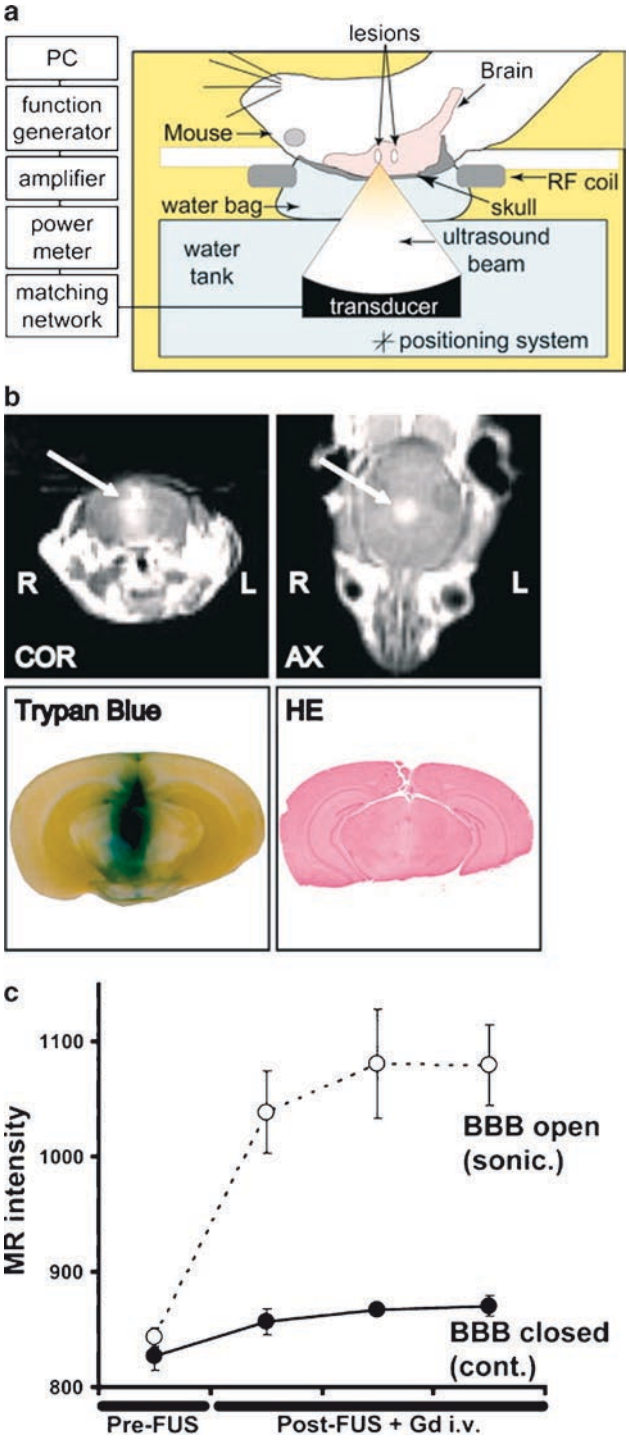
a
PC
function generator
amplifier
power meter
matching network
lesions
Brain
Mouse
RF coil
water bag
skull
water tank
ultrasound beam
transducer
positioning system
b
R
L
COR
R
L
AX
Trypan Blue
HE
c
MR intensity
1100
1000
900
800
BBB open (sonic.)
BBB closed (cont.)
Pre-FUS
Post-FUS + Gd i.v.

Accuracy in the images is determined by the X-ray dose given to the animal. One concern of micro-CT is therefore radiation dose, which despite not being lethal, may be high enough to induce changes in the immune response and other biological pathways, so that experimental outcomes could be affected (Boone et al. 2004; Ford et al. 2003).

Magnetic Resonance Imaging and Spectroscopy

The principal strengths of magnetic resonance (MR) techniques are noninvasiveness, high spatial resolution – of the order of 100 μm for small rodent studies – and excellent soft tissue contrasting capabilities. The signal is governed by a number of parameters, and this wealth of information renders MR a valuable tool for diagnosis, tissue characterization and in vivo morphometry, for obtaining physiological and functional readouts, and for deriving metabolic and, to some extent, target-specific tissue characteristics.

A major limitation of MR is its low sensitivity, and in general terms, the role of in vivo MR imaging (MRI) and spectroscopy (MRS) in pharmacological research is to study the effects of a drug on tissue morphology, physiology and biochemistry rather than to study the fate of the drug itself in the organism. In other words, MR methods yield primarily pharmacodynamic readouts (Beckmann 2006; Beckmann et al. 2001, 2004; Rudin et al. 1999).

Development of gradient systems with improved design (Dodd and Ho 2002; Leggett et al. 2003), of specialized radiofrequency coils for microimaging (Bilgen 2006; Webb 1997), including cryogenic coils (Darrasse and Ginefri 2003; Ratering et al. 2008; Voehler et al. 2006), and of devices for appropriate anesthesia and physiological control (Brau et al. 2004; Hedlund et al. 2000) are significantly improving the quality of mouse MRI/S. Most of the studies are performed at high magnetic fields (≥4.7 T), however, an interesting alternative for translational purposes could be the use of cryogenic coils in combination with magnets operating at lower fields (≤1.5 T), compatible with clinical settings (Poirier-Quinot et al. 2008) (Fig. 3). Despite the practical challenges in performing MRS studies in living mice [see (Choi et al., 2003; Heerschap et al. 2004) for reviews], several groups have shown the feasibility of applying the technique on a routine manner in the neuroscience area (Jenkins et al. 2005; Marjanska et al. 2005; von Kienlin et al. 2005). High resolution proton spectra from the mouse brain can be obtained at high (9.4 T) (Miyasaka et al. 2006; Tkac et al. 2004) and low fields (2.35 T) as well (Schwarcz et al. 2003).

Positron Emission Tomography

Positron Emission Tomography (PET) produces images of the body by detecting the radiation emitted from substances injected into the body and labeled with positron emitting radioactive isotopes such as carbon-11, fluorine-18, oxygen-15,

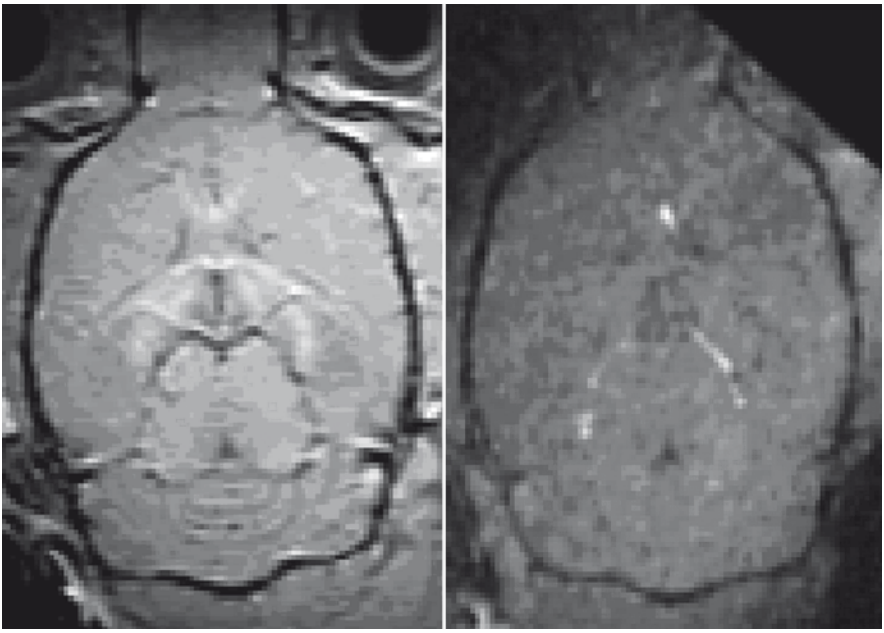

Fig. 3 A MRI of the mouse brain in vivo using a high temperature superconducting radiofrequency coil (*left*) and a conventional copper coil of the same geometry (*right*), both operating at 1.5 T in a clinical scanner. Acquisitions were performed using a gradient-echo sequence. See Poirier-Quinot et al. (2008) for details. Courtesy of Marie Poirier-Quinot, Jean-Christophe Ginefri and Luc Darrasse, Université de Paris Sud – CNRS, Orsay, France

or nitrogen-13. As isotopic substitution does not affect the physicochemical and binding properties of a compound, PET is the method of choice for pharmacokinetic studies of biologically active compounds, for instance drugs or drug candidates, by labeling them with e.g. carbon-11. The short half-life of PET radionuclides implies that scanners have to be located near particle accelerators (cyclotrons) that produce the radioisotopes. PET imaging is one of the most sensitive imaging approaches and picomolar amounts of radiolabel can be readily detected and quantified in vivo, irrespective of tissue depth. For comparison, SPECT and MRI require respectively 10^1–10^2 and 10^7–10^8 higher amounts of probe. Recent advances in radionuclide labeling allow the design and development of a large variety of radiopharmaceuticals including macromolecular structures (Duatti 2004). The availability of such tools enables target-specific studies of label biodistribution, pharmacokinetics, and excretion to be carried out in vivo, as well as to visualize and quantify target expression levels and target function.

Preclinical studies using small laboratory animals demand high spatial resolution provided by dedicated micro-PET systems. Typical voxel volumes achieved with such systems are between $(1.1\ \text{mm})^3$ and $(1.5\ \text{mm})^3$, rendering them adequate for studies in mice, rats, and nonhuman primates (Tay et al. 2005; Weber and Bauer 2004; Yang et al. 2004).

Single Photon Emission Computed Tomography

Single Photon Emission Computed Tomography (SPECT) radionuclides (xenon-133, technetium-99, iodine-123) are characterized by relatively long half-lives. They stabilize by emission of single gamma rays. SPECT is used to collect physiological information (e.g., blood flow) and to measure the biodistribution of radioactive substances. In addition to being less expensive than PET, a SPECT instrument does not need to be located close to a particle accelerator. Commercial small animal SPECT systems capable of measuring mice, typically use pixelated crystal arrays coupled to position sensitive photomultiplier tubes and a pinhole collimator (Beekman et al. 2002; Cao et al. 2005).

In Vivo Optical Imaging

Bioluminescence

Bioluminescence refers to the generation of (visible) light by living organisms, commonly due to an enzymatic reaction (Contag et al. 1997; Zhang et al. 2001). Reporter genes are used to study the expression of a gene of interest. This is achieved by inserting into the host cell genome a gene cassette containing the reporter gene construct under the control of the target gene. Bioluminescent reporters yield exquisite sensitivity as there is no endogenous background signal in mammalian cells resulting in high signal-to-background ratios: using sensitive detection devices such as photomultiplier tubes or cooled charge-coupled devices (CCD) sensitivity is sufficient to count only a few emitted photons.

A prerequisite for bioluminescence imaging is genetic engineering of the tissue cells of interest, i.e. the incorporation of an exogenous reporter gene. The most commonly used bioluminescent reporter is luciferase from the North American firefly that catalyze the transformation of D-luciferin (injected e.g. intraperitoneally) into oxyluciferin in the presence of both O_2 and Mg^{2+}-ATP leading to the emission of radiation at wavelengths larger than 600 nm (Rice et al. 2001), which falls into the window of reduced tissue absorption. Reporter gene assays have been demonstrated to yield fundamental biological information on e.g. transcriptional regulation, signal transduction, protein-protein interactions, cell trafficking or targeted drug action (Choy et al. 2003; Piwnica-Worms et al. 2004).

Fluorescence Imaging

Related to bioluminescence imaging is fluorescence imaging, an attractive tool due to its operational simplicity, safety, and cost-effectiveness. Exogenous fluorochromes (dyes or genetically engineered fluorescent proteins) are excited by e.g. laser diodes operating at a frequency close to that of the detected light; the emitted fluorescent light is then detected in a spatially resolved manner by a CCD camera.

The near-infrared window is particularly suitable for in vivo investigations. Near-infrared fluorescence (NIRF) imaging takes advantage of the low absorbance of tissue chromophores such as oxy- and deoxy-hemoglobin, water, melanin and fat, for light of wavelengths between 650 and 900 nm, to study in vivo biological processes at the cellular and molecular levels. At these wavelengths scattering of photons is a more significant attenuation factor than absorption.

A difficulty of in vivo optical imaging in general, is spatial resolution: the light intensity distribution measured at the surface critically depends on the depth of the light source within the tissue. A population of luciferase-expressing cells near the surface of the skin will appear both brighter and more focused than the same number of cells growing at deeper tissue sites. Tomographic approaches are being devised to improve data quantification (Ntziachristos et al. 2005; Wang et al. 2004; Zacharakis et al. 2005).

Multimodality Imaging

In many respects the imaging techniques discussed above are complementary; there is no "all-in-one" imaging modality providing optimal sensitivity, specificity and temporo-spatial resolution. Due to its relatively low sensitivity, MRI is of limited value for detecting molecular processes in vivo; nevertheless, its high spatial resolution provides a good anatomical reference for molecular data obtained with high sensitivity, low resolution imaging modalities. This might be achieved by postprocessing of data obtained in different imaging sessions or by simultaneous multimodality small animal imaging such as PET-MRI (Benveniste et al. 2005; Lucas et al. 2006; Pichler et al. 2006; Raylman et al. 2007; Slates et al. 1999), PET-CT (Del Guerra and Belcari 2002; Deroose et al. 2007; Hsu et al. 2008; Nahrendorf et al. 2008) and SPECT-CT (Merron et al. 2007; Müller et al. 2008; Seo et al. 2007). Combining imaging data requires compatibility of data formats for the various modalities as well as sophisticated software tools for image coregistration (fusion), data visualization and integration across modalities. The integration of multimodal imaging information into bioinformatics platforms comprising nonimaging data (gene/protein expression data, pharmacodynamic, pharmacokinetic, and pharmacogenetic databases, histological data, atlases) will be mandatory in the future for handling the ever increasing complexity of biomedical information.

Contrast Agents, Molecular Probes and Tracers

For ultrasound, CT and MRI, the administration of exogenous agents serves to enhance the quality of anatomical data or to provide additional information, usually related to the measurement of physiological parameters. On the other hand, for optical imaging and PET/SPECT an imaging agent is a necessity for signal generation. There are two main interests to develop a target-specific contrast agent or tracer in the context of drug discovery:

- Imaging and measuring the drug biodistribution: Early information on drug biodistribution and pharmacokinetic properties is essential during lead optimization and profiling. Conventionally, such data are obtained in rodents by blood and tissue sampling, or by autoradiography. More recently, nuclear imaging methods, in particular PET/micro-PET (Fischman et al. 2002; Phelps 2000), have been regularly used to derive such information in humans and animals as isotopic substitution with 11C or 18F does not affect the physicochemical properties of the compound (Fischman et al. 2002; Phelps 2000). Alternatively, one could label molecules with fluorochromes and use the far more accessible optical imaging techniques as preliminary, fast readouts of drug biodistribution. Compounds selected at this preliminary step would then be submitted to the significantly more involved PET examinations. This approach might be limited to visualize the distribution of large molecular weight compounds such as biopolymers [e.g. monoclonal antibodies (mAb), proteins, siRNA] as the reporter groups for optical imaging are bulky dyes that may affect the properties of the labeled molecule. This influence will be less pronounced on these macromolecules compared to conventional small molecule drugs;
- Imaging the target distribution/density and pharmacodynamic effects of drugs: Demand is for specific reporter probes and amplification strategies in order to differentiate target information from nonspecific background signal and to cope with the low (subnanomolar) target concentrations. Minimization of background signals requires elimination of the unbound and possibly of the nonspecifically bound fraction of the label, which implies a waiting period following injection of the reporter probe. Modulations of the signal from the reporter probe after administration of a drug candidate can be used to assess the compound binding to the target (receptor occupancy) or the effect of the drug on a certain molecular pathway. Reporter probes include targeted agents [e.g. small molecules, peptides, metabolites, antibodies or other molecules labeled with (a) 11C and 18F for PET, (b) ^{111}In or ^{99m}Tc for nuclear imaging, (c) fluorochromes for optical imaging or (d) magnetic reporter probes and activatable probes (Hogemann et al. 2002; Sipkins et al. 1998; Weissleder et al. 2000)]. The latter undergo chemical or physicochemical changes upon interacting with their target. Examples include caged near-infrared fluorochromes (Bornhop et al. 2001; Weissleder and Ntziachristos 2003), protease-activatable dequenching probes (Tung et al. 2000), paramagnetic agents that change spin–lattice relaxivity on activation (Louie et al. 2000), and superparamagnetic sensors (Perez et al. 2002).

Despite the poor sensitivity of MRI there is plenty of evidence that molecular imaging approaches using targeted contrast can become a routine tool for in vivo pharmacological studies in the near future. This requires that a “hot spot” of paramagnetic or superparamagnetic centers be delivered efficiently to the target, which can be achieved by using labeled nanoparticle platforms conjugated to targeting vectors (Lanza et al. 2004; Morawski et al. 2005). These platforms are optimized by different surface modification techniques to have reasonable circulation times to

reach their targets in the tissue by escaping the organism's particle filter (reticuloendothelial system). Among others, lipid-based nanoparticles, such as liposomes or micelles, extensively used as drug carrier vehicles, constitute a promising strategy for molecular imaging applications using MRI [see (Mulder et al. 2006) for a recent review]. Targeting ligands can be conjugated to lipidic particles by incorporating lipids with a functional moiety to allow a specific interaction with molecular markers and to achieve accumulation of the particles at diseased sites.

Reporter molecules for optical imaging consist of a near-infrared fluorescent dye, which can be coupled to target specific ligands/carriers such as antibodies, nanoparticles or polymers, proteins, peptides and small molecules, analogous to radiolabeling methods but with certain limitations due to the bulky dye molecules (Frangioni 2003; Licha 2002). In addition, fluorescence detection allows researchers to design smart sensor reporters based on fluorescence quenching mechanisms, which are not detectable in their native state but are activated by interaction with their target (e.g. protease sensors) to increase signal-to-background ratios (Funovics et al. 2003). Another way to increase the sensitivity of detection is the introduction of biocompatible superbright quantum dots into small animal research (Ballou et al. 2004; Gao et al. 2004) [see (Portney and Ozkan 2006) for a review]. Quantum dots of different colors tuned to target different biological process by coupling to corresponding carrier molecules will potentially enable multiplexed imaging in vivo.

Imaging of Mouse Models of Alzheimer's Disease

In this section, we select imaging of mouse models of Alzheimer's disease (AD) to illustrate issues of particular relevance within the pharmaceutical research context. Pathological features of AD are amyloid-beta (Aβ)-peptide-containing plaques, neurofibrillary tangles consisting of aggregated, hyperphosphorylated tau, extensive neuritic degeneration, and distinct neuron loss. Vascular abnormalities coexist commonly with the histological features of AD (de la Torre 2002; Farkas and Luiten 2001; Iadecola 2004). Deposition of Aβ-peptide in cerebral vessel walls, known as cerebral amyloid angiopathy (CAA), is very frequent, but its contribution to the onset of dementia is unknown (Castellani et al. 2004; Nicoll et al. 2004).

Diagnosing AD remains an imperfect science. No definitive biomarker is currently available (Thal et al. 2006) and this hampers clinical diagnosis and drug discovery involving transgenic mice modeling AD. Various quantitative MR techniques that measure the anatomical, biochemical, microstructural, functional and blood-flow changes are being evaluated as possible surrogate measures of disease progression (Kantarci 2005; Mueggler 2006).

Quantitative volumetry based on MRI is an important approach to assess the disease progression in patients. Correlation between antemortem MRI assessments of the hippocampal volume and postmortem analyses suggest that the hippocampal atrophy, although not specific for AD, is a fairly sensitive marker of both the pathologic stage and the hippocampal neurofibrillary tangle burden (Silbert et al. 2003).

Reduced hippocampal volume and corpus callosum length were detected by MRI in PDAPP mice before Aβ deposition, suggesting that overexpression of APP and amyloid may initiate pathologic changes before the appearance of plaques (Redwine et al. 2003).

Amyloid deposits may affect diffusion properties of the brain interstitium with implications for the transport of endogenous signaling molecules during synaptic and/or extrasynaptic transmission. Using diffusion-weighted MRI, Mueggler et al. (2003b) showed that fibrillar amyloid deposits and associated gliosis in brains of 25-month-old APP23 transgenic mice were accompanied by a reduction in the apparent diffusion coefficient (ADC). This decrease was most pronounced in neocortical areas with a high percentage of congophilic amyloid and was not significant in the caudate putamen, an area with only modest and diffuse amyloid deposition (Fig. 4). These findings suggest that extracellular deposition of fibrillar amyloid and/or associated glial proliferation and hypertrophy cause restrictions to interstitial fluid diffusion. Reduced diffusivity within the interstitial space may alter volume transmission and therefore contribute to the cognitive impairment in AD.

MRI approaches to analyze functional or hemodynamic changes related to the development of AD have also been successful in the process of characterizing transgenic mice in vivo. Functional MRI (fMRI) has been applied to assess brain functionality (Mueggler et al. 2002, 2003b) in APP23 mice. The cerebral hemodynamic response to infusion of the GABAA antagonist, bicuculline, was significantly reduced in aged APP23 mice compared with age-matched wild-type littermates. The decreased response was attributed to a compromised cerebrovascular reactivity associated with perivascular amyloid deposition. For fMRI, not a trivial procedure in small rodents, mice need special preparation (intubation, artificial ventilation, paralysis) which can be a substantial burden especially to aged animals. In addition, the throughput of the experiment is low. Despite providing only semiquantitative information, MR angiography of the mouse brain (Beckmann et al. 1999; Beckmann 2000), performed in spontaneously respiring animals and without administration of contrast material, has proven to be an interesting alternative for analyzing the vascular changes in transgenic mice. High resolution MR angiograms acquired in 16 min demonstrated flow perturbations in major arteries at the Circle of Willis in old but not in young APP23 transgenic mice (Beckmann et al. 2003; Thal et al. 2008). Corrosion casts (Krucker et al. 2004, 2006; Meyer et al. 2008) revealed that, at sites where flow voids were detected in vivo, vessel elimination, substitution and/or deformation had taken place. The loss of vascular integrity revealed by angiography might provide the basis for the age-related impairment of the cerebral blood volume response to pharmacological stimulation in the fMRI studies. Also, changes in relative cerebral blood volume (rCBV) and flow (CBF) determined with ^{2}H MRS and gradient-echo contrast enhanced MRI were reported recently in the brains of APP/PS1 mice subjected to different lipid diets (Hooijmans et al. 2007). Overall, these results support the idea that cerebral microcirculatory abnormalities evolving progressively could contribute to AD pathogenesis and cognitive impairment.

The most consistently reported neurochemical abnormality detected by ^{1}H-MRS in humans is a decrease in *N*-acetylaspartate (NAA) [for reviews see (Kantarci et al.

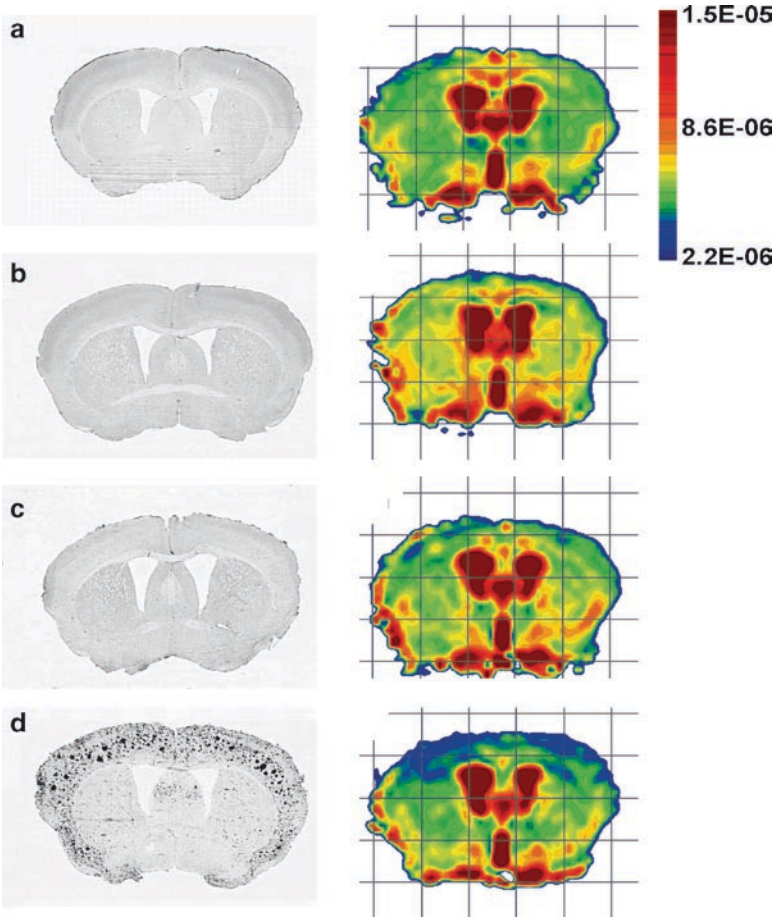

Fig. 4 Color-coded representative ADC maps of a coronal brain section at the level of Bregma for a 6- (C) and 25-month-old APP23 mouse (D) and age-matched controls (6 months, A; 25 months, B). The ADC scale on the right is in 10^{-6} cm^2/s. A significant ADC decline, color-coded in blue, is detectable in the medial and dorso-lateral cortex of aged APP23 mice. In the dorso-lateral cortex of the 6-month-old APP23 mouse, few areas with reduced ADC are visible. Courtesy of Thomas Mueggler, ETH Zurich, Switzerland. Modified with permission from Mueggler et al. (2003a). © Federation of European Neuroscience Societies

2004; Kantarci 2005)], considered as an indicator of neuronal number and health. An increase of the signal from myo-inositol, which may either be a marker for osmotic stress or astrogliosis, has also been reported in AD patients. Thus, myo-inositol may be an earlier marker of pathological change in AD than NAA. Proton MRS has also been applied to transgenic mice in AD research (Marjanska et al. 2005; von Kienlin et al. 2005), with spectral acquisition times between 10 and 35 min. A reduction in NAA and glutamate levels, compared with total creatine levels, and an increase in the concentration of myo-inositol was found in transgenic

mice with advancing age. The spectroscopic measures in vivo correlated well with the plaque load in the frontal cortex.

The ultimate readout of AD would be the visualization of cerebral plaques in vivo. Several groups have pursued the detection of amyloid plaques with MR microimaging in mice without administering contrast media (Braakman et al. 2006; Dhenain et al. 2002, 2007; Helpern et al. 2004; Jack et al. 2005; Lee et al. 2004). Initial trials involved very long acquisition times, up to several hours, however, recently, plaques have been resolved in vivo and at high magnetic fields (≥7 T) in shorter measurement times of the order of 2 h (Jack et al. 2005; Lee et al. 2004) and even of 25 min (Braakman et al. 2006). Another approach involved enhancing contrast-to-noise by using molecular probes that specifically target Aβ plaques (Higuchi et al. 2005; Kandimalla et al 2007; Poduslo et al. 2002; Wadghiri et al. 2003). From the perspective of drug research, these approaches are hampered by either relatively long acquisition times – several hours (Higuchi et al. 2005; Poduslo et al. 2002) – or by the necessity to open the BBB by mannitol (Wadghiri et al. 2003). However, Gd[N-4ab/Q-4ab]Abeta 30, a novel MRI agent based on a derivative of human Aβ peptide shown to cross the blood–brain barrier (BBB) and bind to amyloid plaques in APP/PS1 mice, holds promise for shorter acquisition times (Kandimalla et al. 2007).

Reduced T2 and T2* values have been reported in plaque-like structures in the cortex and hippocampus in several mouse models of AD (Braakman et al. 2006; El Tannir El Tayara et al. 2006; El Tayara Nel et al. 2007; Falangola et al. 2007; Helpern et al. 2004; Vanhoutte et al. 2005). This reduction could be explained by the presence of iron in plaques (Falangola et al. 2005). Despite not detecting plaques directly, this could potentially provide an interesting readout for following with a reasonable throughput age-related plaque load in AD models. A decreasing trend for T2 with age, while plaque area, number and size increased markedly, has been described (Braakman et al. 2006; El Tayara Nel et al. 2007).

Much more sensitive PET and NIRF approaches were successfully applied to detect plaques in vivo. For instance, the Pittsburgh Compound-B (PIB; [11C]6-OH-BTA-1), a hydroxylated derivative of an amyloid-binding dye thioflavin-T, has been developed as a PET tracer for plaque detection in the clinics (Klunk et al. 2004; Mathis et al. 2003). Recently, Maeda et al. (2007) showed the feasibility of quantitatively mapping by micro-PET the amyloid accumulation in the brain of APP23 mice modeling AD using [^{11}C]PIB (Fig. 5). Micro-PET investigations of transgenic mice over an extended range of ages, including longitudinal assessments, demonstrated an age-dependent increase in radioligand binding consistent with progressive amyloid accumulation. The approach has then been used to test therapeutic approaches for AD in APP23 mice. A reduction in amyloid levels has been observed in the hippocampus of transgenic mice during the course of antiamyloid treatment using an antibody against Aβ peptide. Moreover, micro-PET scans with [^{18}F]fluoroethyl-DAA1106, a radiotracer for activated glia, were conducted parallel to amyloid imaging, revealing treatment-induced neuroinflammatory responses, the magnitude of which intimately correlated with the levels of preexisting amyloid estimated by [^{11}C]PIB (Maeda et al 2007). Surprisingly, no signifi-

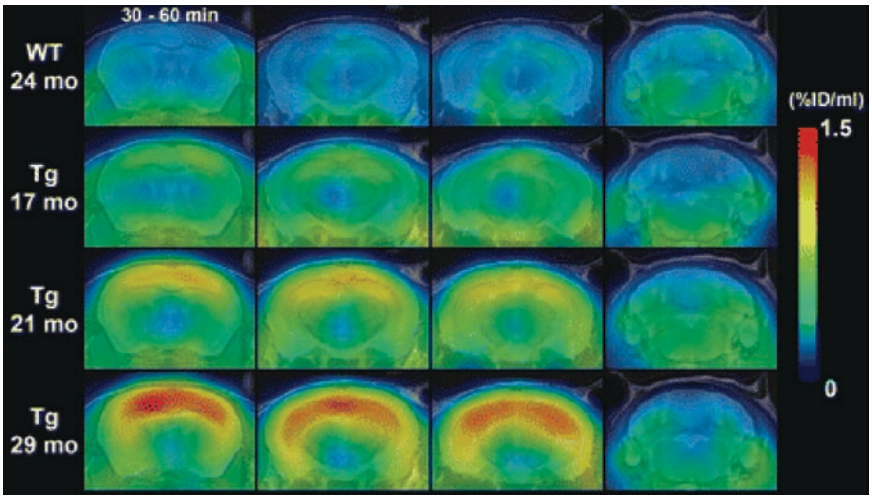

Fig. 5 In vivo detection of amyloid plaques in APP23 mice at different ages. PET images were generated by averaging dynamic scan data at 30–60 min after administration of [^{11}C]PIB and were overlaid on the MRI template. From *left* to *right*, panels represent coronal images at 0, 2, 3, and 7 mm posterior to the bregma. mo, Month. Courtesy of Makoto Higuchi, National Institute of Radiological Sciences, Chiba, Japan. Reproduced with permission from Maeda et al. (2007). © 2007 Society for Neuroscience

cant retention of [^{11}C]PIB was seen in other mouse models, e.g. in presenilin-1/amyloid precursor protein (PS1/APP) (Klunk et al. 2005) and in Tg2576 animals (Toyama et al. 2005) despite an excellent brain uptake of the probe. Possible reasons for this discrepancy could be differences in the secondary structure of Aβ for the transgenic lines.

A NIRF oxazine dye, AOI987, has been demonstrated to readily penetrate the intact BBB and to bind to amyloid plaques (Hintersteiner et al. 2005). Using NIRF imaging, a specific interaction of AOI987 with amyloid plaques was shown in APP23 mice in vivo, and confirmed by postmortem analysis of brain slices. Quantitative analysis revealed increasing fluorescence signal intensity with increasing plaque load of the animals, and significant binding of AOI987 was observed for APP23 transgenic mice aged 9 months and older. Thus, AOI987 is an attractive probe to monitor noninvasively disease progression in animal models of AD and to evaluate the effects of potential drugs on the plaque load.

Final Remarks

Three main roles can be defined for noninvasive mouse imaging in preclinical research (a) phenotyping transgenic animals developed as disease models or for target selection/validation; (b) performing in vivo validation of pharmacological

targets; and (c) testing compounds in murine models of diseases. In all cases, the noninvasive nature of imaging can be exploited to either cope with the high variability in transgenic animal models, or to reduce the biological variability in the pharmacological experiments since the same animal may be used as its own control.

Ideally, an animal imaging laboratory in a pharmaceutical environment should provide access to several techniques. The opportunity to apply a diverse range of imaging techniques to a given problem is a strength. The complementarity of the techniques should be explored to address questions of pharmacological relevance. The choice of technique will be dictated by several factors, including e.g. its spatial and temporal resolution, sensitivity, or availability in clinical diagnosis as well. As a rule, imaging should provide robust and reproducible readouts, and measurements should interfere minimally with the animal's physiology since in most cases repetitive acquisitions are required. Because of the unique challenges encountered in imaging small rodents, not only a thorough understanding of the imaging modality but also of the animal's physiology and the biological/pharmacological question to be addressed is required. Colby and Morenko (2004) have recently addressed several important aspects in small rodent bioimaging, including the choice of appropriate anesthetic regimens, monitoring and supporting the animal's physiologic balance, biosecurity and radiation safety.

A fundamental driving force behind activities involving the use of imaging to characterize animal models of human disease in drug discovery is that the methods may facilitate the translation between preclinical and clinical drug research and development. Once potential biomarkers are identified and validated (qualified), similar study designs can be applied to preclinical and clinical investigations involving a given compound. Moreover, studies in animals can serve as the basis to rationalize experimental findings in humans through the use of analogous biomedical readouts. Helping to bridge the two intimately connected, however in practice often too distant, areas of preclinical and clinical research is a major contribution of imaging in pharmaceutical research.

References

Acton PD, Kung HF (2003) Small animal imaging with high resolution single photon emission tomography. Nucl Med Biol 30:889–895

Badea C, Hedlund LW, Johnson GA (2004) Micro-CT with respiratory and cardiac gating. Med Phys 31:3324–3329

Ballou B, Lagerholm BC, Ernst LA et al (2004) Noninvasive imaging of quantum dots in mice. Bioconjug Chem 15:79–86

Beckmann N (2000) High resolution magnetic resonance angiography non-invasively reveals mouse strain differences in the cerebrovascular anatomy in vivo. Magn Reson Med 44:252–258

Beckmann N (2006) In vivo MR techniques in drug discovery and development. . New York, Taylor & Francis

Beckmann N, Stirnimann R, Bochelen D (1999) High-resolution magnetic resonance angiography of the mouse brain: application to murine focal cerebral ischemia models. J Magn Reson 140:442–450

Beckmann N, Mueggler T, Allegrini PR et al (2001) From anatomy to the target: contributions of magnetic resonance imaging to preclinical pharmaceutical research. Anat Rec 265:85–100

Beckmann N, Schuler A, Mueggler T et al (2003) Age-dependent cerebrovascular abnormalities and blood flow disturbances in APP23 mice modeling Alzheimer's disease. J Neurosci 23:8453–8459

Beckmann N, Tigani B, Laurent D et al (2004) Magnetic resonance imaging in drug discovery: lessons from disease areas. Drug Discov Today 9:35–42

Beekman FJ, McElroy DP, Berger F et al (2002) Towards in vivo nuclear microscopy: iodine-125 imaging in mice using micro-pinholes. Eur J Nucl Med Mol Imaging 29:933–938

Benveniste H, Fowler JS, Rooney W et al (2005) Maternal and fetal 11C-cocaine uptake and kinetics measured in vivo by combined PET and MRI in pregnant nonhuman primates. J Nucl Med 46:312–320

Bilgen M (2006) Inductively-overcoupled coil design for high resolution magnetic resonance imaging. Biomed Eng Online 5:3

Boone JM, Velazquez O, Cherry SR (2004) Small-animal X-ray dose from micro-CT. Mol Imaging 3:149–158

Bornhop DJ, Contag CH, Licha K et al (2001) Advance in contrast agents, reporters, and detection. J Biomed Opt 6:106–10

Braakman N, Matysik J, van Duinen SG et al (2006) Longitudinal assessment of alzheimer's β-amyloid plaque development in transgenic mice monitored by in vivo magnetic resonance microimaging. J Magn Reson Imaging 24:530–536

Brau AC, Hedlund LW, Johnson GA (2004) Cine magnetic resonance microscopy of the rat heart using cardiorespiratory-synchronous projection reconstruction. J Magn Reson Imaging 20:31–38

Cao Z, Bal G, Accorsi R, Acton PD (2005) Optimal number of pinholes in multi-pinhole SPECT for mouse brain imaging – a simulation study. Phys Med Biol 50:4609–4624

Castellani RJ, Smith MA, Perry G et al (2004) Cerebral amyloid angiopathy: major contributor or decorative response to Alzheimer's disease pathogenesis. Neurobiol Aging 25:599–602

Cavanaugh D, Johnson E, Price RE et al (2004) In vivo respiratory-gated micro-CT imaging in small-animal oncology models. Mol Imaging 3:55–62

Chen XJ, Henkelman RM (2006) Rapid phenotyping of mice with MRI. In: Beckmann N (ed) In vivo MR techniques in drug discovery and development. Taylor & Francis, New York, pp 75–92

Choi IY, Lee SP, Guilfoyle DN et al (2003) In vivo NMR studies of neurodegenerative diseases in transgenic and rodent models. Neurochem Res 28:987–1001

Choi JJ, Pernot M, Small SA et al (2007) Noninvasive, transcranial and localized opening of the blood–brain barrier using focused ultrasound in mice. Ultra-sound Med Biol 33:95–104

Choy G, Choyke P, Libutti SK (2003) Current advances in molecular imaging: noninvasive in vivo bioluminescent and fluorescent optical imaging in cancer research. Mol Imaging 2:303–312

Colby LA, Morenko BJ (2004) Clinical considerations in rodent bioimaging. Comp Med 54:623–630

Contag CH, Bachmann MH (2002) Advances in in vivo bioluminescence imaging of gene expression. Annu Rev Biomed Eng 4:235–260

Contag CH, Spilman SD, Contag PR et al (1997) Visualizing gene expression in living mammals using a bioluminescent reporter. Photochem Photobiol 66:523–531

Darrasse L, Ginefri JC (2003) Perspectives with cryogenic RF probes in biomedical MRI. Biochimie 85:915–937

de la Torre JC (2002) Alzheimer disease as a vascular disorder: nosological evidence. Stroke 33:1152–1162

Del Guerra A, Belcari N (2002) Advances in animal PET scanners. Q J Nucl Med 46:35–47

Deroose CM, De A, Loening AM et al (2007) Multimodality imaging of tumor xenografts and metastases in mice with combined small-animal PET, small-animal CT, and bioluminescence imaging. J Nucl Med 48:295–303

Dhenain M, El Tannir El Tayara N, Wu TD et al (2007) Characterization of in vivo MRI detectable thalamic amyloid plaques from APP/PS1 mice. Neurobiol Aging 30:41–53

Dhenain M, Privat N, Duyckaerts C et al (2002) Senile plaques do not induce susceptibility effects in T2*-weighted MR microscopic images. NMR Biomed 15:197–203

Dodd SJ, Ho C (2002) Short planar gradient coils for MR microscopy using concentric return paths. J Magn Reson 156(1):1–9

Duatti A (2004) In vivo imaging of oligonucleotides with nuclear tomography. Curr Drug Targets 5:753–760

El Tannir El Tayara N, Delatour B, Le Cudennec C et al (2006) Age-related evolution of amyloid burden, iron load, and MR relaxation times in a transgenic mouse model of Alzheimer's disease. Neurobiol Dis 22:199–208

El Tayara Nel T, Volk A, Dhenain M (2007) Delatour B.Transverse relaxation time reflects brain amyloidosis in young APP/PS1 transgenic mice. Magn Reson Med 58:179–184

Falangola MF, Lee SP, Nixon RA et al (2005) Histological co-localization of iron in Abeta plaques of PS/APP transgenic mice. Neurochem Res 30:201–205

Falangola MF, Dyakin VV, Lee SP et al (2007) Quantitative MRI reveals aging-associated T2 changes in mouse models of Alzheimer's disease. NMR Biomed 20:343–351

Farkas E, Luiten PG (2001) Cerebral microvascular pathology in aging and Alzheimer's disease. Prog Neurobiol 64:575–611

Fischman AJ, Alpert NM, Rubin RH (2002) Pharmacokinetic imaging: a noninvasive method for determining drug distribution and action. Clin Pharmacokinet 41:581–602

Ford NL, Thornton MM, Holdsworth DW (2003) Fundamental image quality limits for micro-computed tomography in small animals. Med Phys 30:2869–2877

Ford NL, Nikolov HN, Norley CJ et al (2005) Prospective respiratory-gated micro-CT of free breathing rodents. Med Phys 32:2888–2898

Frangioni JV (2003) In vivo near-infrared fluorescence imaging. Curr Opin Chem Biol 7:626–634

Funovics M, Weissleder R, Tung CH (2003) Protease sensors for bioimaging. Anal Bioanal Chem 377:956–963

Gambhir SS (2002) Molecular imaging of cancer with positron emission tomography. Nat Rev Cancer 2:683–693

Gao X, Cui Y, Levenson RM et al (2004) In vivo cancer targeting and imaging with semiconductor quantum dots. Nat Biotechnol 22:969–976

Hammoud DA, Hoffman JM, Pomper MG (2007) Molecular neuroimaging: From conventional to emerging techniques. Radiology 245:21–42

Hedlund LW, Cofer GP, Owen SJ et al (2000) MR-compatible ventilator for small animals: computer-controlled ventilation for proton and noble gas imaging. Magn Reson Imaging 18:753–759

Heerschap A, Sommers MG in 't Zandt HJ et al (2004) Nuclear magnetic resonance in laboratory animals. Methods Enzymol 385:41–63

Helpern JA, Lee SP, Falangola MF et al (2004) MRI assessment of neuropathology in a transgenic mouse model of Alzheimer's disease. Magn Reson Med 51:794–798

Higuchi M, Iwata N, Matsuba Y et al (2005) 19F and 1H MRI detection of amyloid beta plaques in vivo. Nat Neurosci 8:527–533

Hintersteiner M, Enz A, Frey P et al (2005) In vivo detection of amyloid-β deposits by near-infrared imaging using an oxazine-derivative probe. Nat Biotechnol 23:577–583

Hogemann D, Ntziachristos V, Josephson L et al (2002) High throughput magnetic resonance imaging for evaluating targeted nanoparticle probes. Bioconjug Chem 13:116–121

Hooijmans CR, Rutters F, Dederen PJ et al (2007) Changes in cerebral blood volume and amyloid pathology in aged Alzheimer APP/PS1 mice on a docosahexaenoic acid (DHA) diet or cholesterol enriched Typical Western Diet (TWD). Neurobiol Dis 28:16–29

Hsu WK, Virk MS, Feeley BT et al (2008) Characterization of osteolytic, osteoblastic, and mixed lesions in a prostate cancer mouse model using 18F-FDG and 18F-fluoride PET/CT. J Nucl Med 49:414–421

Iadecola C (2004) Neurovascular regulation in the normal brain and in Alzheimer's disease. Nat Rev Neurosci 5:347–360

Jack CR Jr, Wengenack TM, Reyes DA et al (2005) In vivo magnetic resonance microimaging of individual amyloid plaques in Alzheimer's transgenic mice. J Neurosci 25:10041–10048

Jenkins BG, Andreassen OA, Dedeoglu A et al (2005) Effects of CAG repeat length, HTT protein length and protein context on cerebral metabolism measured using magnetic resonance spectroscopy in transgenic mouse models of Huntington's disease. J Neurochem 95:553–562

Kandimalla KK, Wengenack TM, Curran GL et al (2007) Pharmacokinetics and amyloid plaque targeting ability of a novel peptide-based magnetic resonance contrast agent in wild-type and Alzheimer's disease transgenic mice. J Pharmacol Exp Ther 322:541–549

Kantarci K (2005) Magnetic resonance markers for early diagnosis and progression of Alzheimer's disease. Expert Rev Neurother 5:663–670

Kantarci K, Petersen RC, Boeve BF et al (2004) 1H MR spectroscopy in common dementias. Neurology 63:1393–1398

Kinoshita M, Hynynen K (2005) A novel method for the intracellular delivery of siRNA using microbubble-enhanced focused ultrasound. Biochem Biophys Res Commun 335:393–399

Kinoshita M, McDannold N, Jolesz FA et al (2006a) Targeted delivery of antibodies through the blood–brain barrier by MRI-guided focused ultrasound. Biochem Biophys Res Commun 340:1085–1090

Kinoshita M, McDannold N, Jolesz FA et al (2006b) Noninvasive localized delivery of Herceptin to the mouse brain by MRI-guided focused ultrasound-induced blood–brain barrier disruption. Proc Natl Acad Sci USA 103:11719–11723

Klunk WE, Engler H, Nordberg A et al (2004) Imaging brain amyloid in Alzheimer's disease with Pittsburgh compound-B. Ann Neurol 55:306–319

Klunk WE, Lopresti BJ, Ikonomovic MD et al (2005) Binding of the positron emission tomography tracer Pittsburgh compound-B reflects the amount of amyloid-beta in Alzheimer's disease brain but not in transgenic mouse brain. J Neurosci 25:10598–10606

Krucker T, Schuler A, Meyer EP et al (2004) Magnetic resonance angiography and vascular corrosion casting as tools in biomedical research: application to transgenic mice modeling Alzheimer's disease. Neurol Res 26:507–516

Krucker T, Lang A, Meyer EP (2006) New polyurethane-based material for vascular corrosion casting with improved physical and imaging characteristics. Microsc Res Tech 69:138–147

Lanza GM, Winter P, Caruthers S et al (2004) Novel paramagnetic contrat agents for molecular imaging and targeted drug delivery. Curr Pharm Biotech 5:495–507

Lee SP, Falangola MF, Nixon RA et al (2004) Visualization of beta-amyloid plaques in a transgenic mouse model of Alzheimer's disease using MR microscopy without contrast reagents. Magn Reson Med 52:538–544

Leggett J, Crozier S, Bowtell RW (2003) Actively shielded multi-layer gradient coil designs with improved cooling properties. J Magn Reson 165:196–207

Licha K (2002) Contrast agents for optical imaging. Top Curr Chem 222:1–29

Louie AY, Huber MM, Ahrens ET et al (2000) In vivo visualization of gene expression using magnetic resonance imaging. Nat Biotechnol 18:321–325

Lucas AJ, Hawkes RC, Ansorge RE et al (2006) Development of a combined microPET-MR system. Technol Cancer Res Treat 5:337–341

Maeda J, Ji B, Irie T et al (2007) Longitudinal, quantitative assessment of amyloid, neuroinflammation, and anti-amyloid treatment in a living mouse model of Alzheimer's disease enabled by positron emission tomography. J Neurosci 27:10957–10968

Marjanska M, Curran GL, Wengenack TM et al (2005) Monitoring disease progression in transgenic mouse models of Alzheimer's disease with proton magnetic resonance spectroscopy. Proc Natl Acad Sci USA 102:11906–11910

Mathis CA, Wang Y, Holt DP et al (2003) Synthesis and evaluation of 11C-labeled 6-substituted 2-arylbenzothiazoles as amyloid imaging agents. J Med Chem 46:2740–2754
Merron A, Peerlinck I, Martin-Duque P et al (2007) SPECT/CT imaging of oncolytic adenovirus propagation in tumours in vivo using the Na/I symporter as a reporter gene. Gene Ther 14:1731–1738
Meyer EP, Ulmann-Schuler A, Staufenbiel M et al (2008) Altered morphology and 3D architecture of brain vasculature in a mouse model for Alzheimer's disease. Proc Natl Acad Sci USA 105:3587–3592
Miyasaka N, Takahashi K, Hetherington HP (2006) Fully automated shim mapping method for spectroscopic imaging of the mouse brain at 9.4 T. Magn Reson Med 55:198–202
Morawski AM, Lanza GA, Wickline SA (2005) Targeted contrast agents for magnetic resonance imaging and ultrasound. Curr Opin Biotechnol 16:89–92
Mueggler T (2006) Magnetic resonance imaging and spectroscopy in transgenic mice modelling Alzheimer's disease. In: Beckmann N (ed) Vivo MR techniques in drug discovery and development. Taylor & Francis, New York, pp 95–110
Mueggler T, Sturchler-Pierrat C, Baumann D et al (2002) Compromised hemodynamic response in amyloid precursor protein transgenic mice. J Neurosci 22:7218–7224
Mueggler T, Meyer-Luehmann M, Rausch M et al (2003a) Restricted diffusion in the brain of transgenic mice with cerebral amyloidosis. Eur J Neurosci 20:811–817
Mueggler T, Baumann D, Rausch M et al (2003b) Age-dependent impairment of somatosensory response in the amyloid precursor protein 23 transgenic mouse model of Alzheimer's disease. J Neurosci 23:8231–8236
Mulder WJ, Douma K, Koning GA et al (2006) Liposome-enhanced MRI of neointimal lesions in the ApoE-KO mouse. Magn Reson Med 55:1170–1174
Müller C, Forrer F, Schibli R et al (2008) SPECT study of folate receptor-positive malignant and normal tissues in mice using a novel 99mTc-radiofolate. J Nucl Med 49:310–317
Nahrendorf M, Zhang H, Hembrador S et al (2008) Nanoparticle PET-CT imaging of macrophages in inflammatory atherosclerosis. Circulation 117:379–387
Nicoll JA, Yamada M, Frackowiak J et al (2004) Cerebral amyloid angiopathy plays a direct role in the pathogenesis of Alzheimer's disease. Pro-CAA position statement. Neurobiol Aging 25:589–597
Nieman BJ, Bishop J, Dazai J et al (2007) MR technology for biological studies in mice. NMR Biomed 20:291–303
Ntziachristos V, Bremer C, Weissleder R (2003) Fluorescence imaging with near-infrared light: new technological advances that enable in vivo molecular imaging. Eur Radiol 13:195–208
Ntziachristos V, Ripoll J, Wang LV et al (2005) Looking and listening to light: the evolution of whole-body photonic imaging. Nat Biotechnol 23:313–320
Perez JM, Josephson L, O'Loughlin T et al (2002) Magnetic relaxation switches capable of sensing molecular interactions. Nat Biotechnol 20:816–820
Phelps ME (2000) Positron emission tomography provides molecular imaging of biological processes. Proc Natl Acad Sci USA 97:9226–9233
Pichler BJ, Judenhofer MS, Catana C et al (2006) Performance test of an LSO-APD detector in a 7-T MRI scanner for simultaneous PET/MRI. J Nucl Med 47:639–647
Piwnica-Worms D, Schuster DP, Garbow JR (2004) Molecular imaging of host-pathogen interactions in intact small animals. Cell Microbiol 6:319–331
Poduslo JF, Wengenack TM, Curran GL et al (2002) Molecular targeting of Alzheimer's amyloid plaques for contrast-enhanced magnetic resonance imaging. Neurobiol Dis 11:315–329
Poirier-Quinot M, Ginefri JC, Robert P et al (2008) Performance of a miniature HTS surface coil for in vivo micro-imaging of the mouse in a standard 1.5 T clinical whole-body scanner. Magn Reson Med 60:917–927
Portney NG, Ozkan M (2006) Nano-oncology: drug delivery, imaging, and sensing. Anal Bioanal Chem 384:620–630
Ratering D, Baltes C, Nordmeyer-Massner J et al (2008) Performance of a 200-MHz cryogenic RF probe designed for MRI and MRS of the murine brain. Magn Reson Med 59:1440–1447.

Raylman RR, Majewski S, Velan SS et al (2007) Simultaneous acquisition of magnetic resonance spectroscopy (MRS) data and positron emission tomography (PET) images with a prototype MR-compatible, small animal PET imager. J Magn Reson 186:305–310

Redwine JM, Kosofsky B, Jacobs RE et al (2003) Dentate gyrus volume is reduced before onset of plaque formation in PDAPP mice: a magnetic resonance microscopy and stereologic analysis. Proc Natl Acad Sci USA 100:1381–1386

Rice BW, Cable MD, Nelson MB (2001) In vivo imaging of light-emitting probes. J Biomed Opt 6:432–440

Ritman EL (2004) Micro-computed tomography-current status and developments. Annu Rev Biomed Eng 6:185–208

Rudin M (2006) Molecular imaging. Basic principles and applications in biomedical research. Imperial College Press, London

Rudin M, Beckmann N, Porszasz R et al (1999) In vivo magnetic resonance methods in pharmaceutical research: current status and perspectives. NMR Biomed 12:69–97

Schwarcz A, Natt O, Watanabe T et al (2003) Localized proton MRS of cerebral metabolite profiles in different mouse strains. Magn Reson Med 49:822–827

Seo Y, Gao DW, Hasegawa BH et al (2007) Rodent brain imaging with SPECT/CT. Med Phys 34:1217–1220

Silbert LC, Quinn JF, Moore MM et al (2003) Changes in premorbid brain volume predict Alzheimer's disease pathology. Neurology 61:487–492

Sipkins DA, Cheresh DA, Kazemi MR et al (1998) Detection of tumor angiogenesis in vivo by alphaVbeta3-targeted magnetic resonance imaging. Nat Med 4:623–626

Slates RB, Farahani K, Shao Y et al (1999) A study of artefacts in simultaneous PET and MR imaging using a prototype MR compatible PET scanner. Phys Med Biol 44:2015–2027

Tay YC, Ruangma A, Rowland D et al (2005) Performance evaluation of the microPET focus: a Third-generation micropet scanner dedicated to animal imaging. J Nucl Med 46:455–463

Thal LJ, Kantarci K, Reiman EM et al (2006) The role of biomarkers in clinical trials for Alzheimer disease. Alzheimer Dis Assoc Disord 20:6–15

Thal DR, Capetillo-Zarate E, Larionov S et al (2008) Capillary cerebral amyloid angiopathy is associated with vessel occlusion and cerebral blood flow disturbances. Neurobiol Aging . doi:10.1016/j.neurobiolaging.2008.01.017

Tkac I, Henry PG, Andersen P et al (2004) Highly resolved in vivo 1H NMR spectroscopy of the mouse brain at 9.4 T. Magn Reson Med 52:478–484

Tornell J, Snaith M (2002) Transgenic systems in drug discovery: from target identification to humanized mice. Drug Discov Today 7:461–470

Toyama H, Ye D, Ichise M et al (2005) PET imaging of brain with the beta-amyloid probe, [11C]6-OH-BTA-1, in a transgenic mouse model of Alzheimer's disease. Eur J Nucl Med Mol Imaging 32:593–600

Tung CH, Mahmood U, Bredow S et al (2000) In vivo imaging of proteolytic enzyme activity using a novel molecular reporter. Cancer Res 60:4953–4958

Vanhoutte G, Dewachter I, Borghgraef P et al (2005) Noninvasive in vivo MRI detection of neuritic plaques associated with iron in APP[V717I] transgenic mice, a model for Alzheimer's disease. Magn Reson Med 53:607–613

Voehler MW, Collier G, Young JK et al (2006) Performance of cryogenic probes as a function of ionic strength and sample tube geometry. J Magn Reson 183:102–109

von Kienlin M, Kunnecke B, Metzger F et al (2005) Altered metabolic profile in the frontal cortex of PS2APP transgenic mice, monitored throughout their life span. Neurobiol Dis 18:32–39

Wadghiri YZ, Sigurdsson EM, Sadowski M et al (2003) Detection of Alzheimer's amyloid in transgenic mice using magnetic resonance microimaging. Magn Reson Med 50:293–302

Wang G, Li Y, Jiang M (2004) Uniqueness theorems in bioluminescence tomography. Med Phys 31:2289–2299

Webb AG (1997) Radiofrequency microcoils in magnetic resonance. Progr Nucl Magn Reson Spectrosc 31:1–42

Weber S, Bauer A (2004) Small animal PET: aspects of performance assessment. Eur J Nucl Med Mol Imaging 31:1545–1555

Weissleder R, Ntziachristos V (2003) Shedding light onto live molecular targets. Nat Med 9:123–128

Weissleder R, Moore A, Mahmood U et al (2000) In vivo magnetic resonance imaging of transgene expression. Nat Med 6:351–355

Yang Y, Tai YC, Siegel S et al (2004) Optimization and performance evaluation of the microPET II scanner for in vivo small-animal imaging. Phys Med Biol 49:2527–2545

Zacharakis G, Kambara H, Shih H et al (2005) Volumetric tomography of fluorescent proteins through small animals in vivo. Proc Natl Acad Sci USA 102:18252–18257

Zambrowicz BP, Sands AT (2003) Knockouts model the 100 best-selling drugs – will they model the next 100? Nat Rev Drug Discov 2:38–51

Zambrowicz BP, Turner CA, Sands AT (2003) Predicting drug efficacy: knockouts model pipeline drugs of the pharmaceutical industry. Curr Opin Pharmacol 3:563–570

Zhang W, Feng JQ, Harris SE et al (2001) Rapid in vivo functional analysis of transgenes in mice using whole body imaging of luciferase expression. Transgenic Res 10:423–434